



## Original Article

## Sustained notch signaling inhibition with a gamma-secretase inhibitor prevents traumatic heterotopic ossification



Zheng Wang<sup>a,b,1</sup>, Xinzeyu Yi<sup>a,b,1</sup>, Chao Jian<sup>a,b</sup>, Baiwen Qi<sup>a,b</sup>, Qiaoyun Liu<sup>a,b,\*\*</sup>, Zonghuan Li<sup>a,b,\*\*\*</sup>, Aixi Yu<sup>a,b,\*</sup>

<sup>a</sup> Department of Orthopedics Trauma and Microsurgery, Zhongnan Hospital of Wuhan University, Wuhan, Hubei, China

<sup>b</sup> Hubei Clinical Medical Research Center of Trauma and Microsurgery, Wuhan, Hubei, China

## ARTICLE INFO

## Keywords:

Traumatic heterotopic ossification  
Notch signaling  
Gamma-secretase  
Tissue-resident mesenchymal progenitor cells  
Differentiation  
Proliferation

## ABSTRACT

**Background:** Traumatic heterotopic ossification (THO) is a devastating sequela following traumatic injuries and orthopedic surgeries. To date, the exact molecular mechanism of THO formation is still unclear, which hinders the development of effective treatments. The process of THO formation is believed to recapitulate a series of spatiotemporal cellular and signaling events that occur during skeletal development. The Notch signaling pathway is a critical genetic regulator in embryological bone development and fracture healing. However, few data are available concerning whether Notch signaling regulates THO development and maturation.

**Methods:** We firstly detected the expressions of Notch target genes in both mouse and human THO samples with quantitative RT-PCR and immunohistochemistry (IHC). Then, tissue-resident mesenchymal progenitor cells (TMPCs) were isolated, and the abilities of the proliferation and osteogenic and chondrogenic differentiation of TMPCs were examined under the intervention of the gamma-secretase inhibitor-DAPT at different time points. Finally, DAPT was also administrated in THO mice by burn and Achilles tenotomy injury, and ectopic cartilage and bone formation were monitored by histology and micro-CT.

**Results:** Several Notch target genes were upregulated in both mouse and human THO tissues. Sustained Notch signaling inhibition by DAPT reduced proliferation, osteogenic and chondrogenic differentiation of TMPCs in a time-dependent manner. Moreover, DAPT administration within 3 weeks could inhibit ectopic cartilage and bone formation in a mouse THO model without affecting the total body bone mass.

**Conclusions:** The Notch signaling serves as an important therapeutic target during THO formation. And sustained gamma-secretase inhibition by DAPT has great potential in repressing chondrogenic and osteogenic differentiation of TMPCs, as well as inhibited ectopic cartilage and bone formation *in vivo*.

**The translational potential of this article:** Sustained Notch inhibition via systemic DAPT (or other similar gamma-secretase inhibitors) administration has promising clinical utility for inhibiting THO formation, providing new insight into THO prophylaxis and treatment.

## 1. Introduction

Traumatic heterotopic ossification (THO) is defined as the abnormal formation of bone and cartilage matrix in soft tissues, which may occur in certain predisposing conditions, including arthroplasty, bone fracture or

dislocation, traumatic brain and spinal cord injury, and severe burns [1]. Significant complications associated with THO include chronic pain, impaired prosthetic fitting, decreased range of motion, neurovascular compromise, and skin breakdown, resulting in poor quality of life [2]. Currently, surgical excision of the lesion is the only standard therapeutic

\* Corresponding author. Department of Orthopedics Trauma and Microsurgery, Zhongnan Hospital of Wuhan University, No.169 Donghu Road, Wuhan, Hubei, 430071, China.

\*\* Corresponding author. Department of Orthopedics Trauma and Microsurgery, Zhongnan Hospital of Wuhan University, No.169 Donghu Road, Wuhan, Hubei, 430071, China.

\*\*\* Corresponding author. Department of Orthopedics Trauma and Microsurgery, Zhongnan Hospital of Wuhan University, No.169 Donghu Road, Wuhan, Hubei, 430071, China.

E-mail addresses: [lqy-032529@163.com](mailto:lqy-032529@163.com) (Q. Liu), [lizonghuan@whu.edu.cn](mailto:lizonghuan@whu.edu.cn) (Z. Li), [yuaixi@whu.edu.cn](mailto:yuaixi@whu.edu.cn) (A. Yu).

<sup>1</sup> Zheng Wang and Xinzeyu Yi are co-first authors. These authors contributed equally to this study.

option for symptomatic THO that has already occurred. Unfortunately, surgery is limited by the incomplete restoration of the range of motion and a high recurrence rate [3]. Other prophylactic measures are limited to non-steroidal anti-inflammatory drugs and radiation, which should be administered during the early stages of formation and result in severe complications even in patients who may not eventually develop THO [4].

To date, the exact molecular mechanism of THO formation is still unclear. Although multiple interacting pathways have been identified as vital roles in this process, including TGF- $\beta$ , mTOR, hypoxia-inducible factors (HIF), retinoic acid receptor (RAR), and GNAS signaling pathway [1], no single pathway could fully elucidate the underlying pathological process, which has led to poor efficacy of drugs or gene therapies developed basing on these pathways. THO is often attributed to abnormal proliferation and osteochondral differentiation after acute inflammatory insult with tissue-resident mesenchymal progenitor cells (TMPCs) located in the injury site [5,6]. Histologically, THO is believed to develop through a process of endochondral ossification involving four stages: inflammation, chondrogenesis, osteogenesis, and maturation [1]. Therefore, the process of THO formation recapitulates many programs of embryological bone development and fracture healing [4], suggesting overlapping pathways between bone and THO formation, such as the intimate coupling of Notch signaling pathway and endochondral ossification [7–9].

Notch is an evolutionarily conserved cell–cell signaling pathway that, in mammals, has five ligands (Jagged 1 and 2, and Delta-like ligands 1, 3, and 4) and four receptors (Notch1–4). Upon ligand binding, Notch intracellular domain (NICD) is cleaved by a gamma-secretase complex, then translocates to the nucleus where it binds to RBPjk and mastermind-like (Maml), and activates transcription of downstream target genes, including the Hes and Hey family of transcriptional repressors [10]. Previous data have identified the Notch signaling pathway as a critical genetic regulator of skeletal progenitor cell differentiation, chondrocyte proliferation and maturation, and osteoblast proliferation and maturation in embryological bone development and fracture healing [11,12].

The Notch pathway plays a context-dependent function at different time points within a cell lineage during the process of endochondral ossification, and mechanistic interpretation of transgenic mouse models has been controversial in the field [13]. Early activation of Notch signaling in mesenchymal stem cells (MSCs) promotes cell proliferation and maintains the progenitor pool but also arrests cell differentiation to keep cells in a younger stage [8,9]. However, once MSCs enter the early osteochondral phase, the role of the Notch pathway is dependent on the differentiation stage. In cartilage development, Notch signaling in MSCs might play an inhibitory role during early chondrocyte differentiation but was necessary for chondrocyte hypertrophy [9,14]. An earlier report also suggested that Jag-1-mediated Notch signaling in MSCs was necessary to initiate chondrogenesis, but it must be switched off for chondrogenesis to proceed [15]. In the osteoblast lineage, including the osteochondroprogenitor cell, perichondral cells, preosteoblasts and finally osteoblast, Notch signaling variably exhibits a suppressive or inductive effect [16]. In other studies, Notch signaling suppresses the early and late stages of osteoblastogenesis but induces the intermediate stage [8,17]. However, other reports suggested that mid-to-late activation of Notch drives osteoblast differentiation and promotes the anabolic activity of committed osteoblasts [13,18]. The above evidence implies that the role of Notch signaling during endochondral ossification in embryological bone development and fracture healing is complicated and endogenous Notch signaling may be required for appropriate timing and localization to maintain the delicate balance of bone development and homeostasis.

However, few data are available concerning whether Notch signaling could regulate THO development and maturation. In the present study, we first surveyed the expressions of Notch target genes within the mouse THO model and human THO tissues. Moreover, we investigated the role of Notch signaling in regulating THO by using the gamma-secretase inhibitor-DAPT, to block gamma-secretase-mediated canonical Notch

signaling *in vitro* and *in vivo*.

## 2. Materials and methods

### 2.1. Ethics statement

All animal procedures were performed according to the Guide for the Care and Use of Laboratory Animals of the National Institutes of Health and approved by the Experimental Animal Welfare Ethics Committee of Zhongnan Hospital of Wuhan University (Approval number: ZN2021153). The studies involving human participants were reviewed and approved by the Medical Ethics Committee for Clinical Research Projects of Zhongnan Hospital (Approval number: 2022042K). The patients/participants provided their written informed consent to participate in this study.

### 2.2. Immunohistochemistry (IHC) of human THO samples

THO tissues were obtained from 5 patients in Zhongnan Hospital of Wuhan University, whose demographics are provided in [Supplemental Table S1](#). The regular X-ray examination showed that the formation of THO was in progress. Normal tissues obtained from the same patients away from the THO lesions served as controls. To perform the IHC staining, tissues were embedded in paraffin wax and were sectioned at 5  $\mu$ m. Then, the sections were deparaffinized and re-hydrated. After antigen retrieval, the sections were blocked with 3% bovine serum albumin for 30 min, incubated with an anti-Hey2 or HeyL antibody (Boster, Wuhan, China). The sections were visualized under a light microscope (Olympus, Tokyo, Japan). The average immunoreactivity of the antigen was calculated as the optical density of the antibody in the nucleus/the total nucleus areas  $\times$  100% using the ImageJ software 1.8 (National Institutes of Health, Bethesda, MD, USA).

### 2.3. THO modeling

Seventy male C57BL/6 mice (6-week-old, body weight 18–20 g) were purchased from the Sibeifu Biotechnology Co., Ltd (Beijing, China). Sixty-five mice were subjected to the well-established burn/Achilles' tenotomy injury model to induce THO, as previously described [19]. Briefly, after being anesthetized by intraperitoneal pentobarbital sodium (1%, 5 mL/kg; Sigma-Aldrich, MO, USA), the Achilles tendon was exposed and sharply severed at the midpoint. Then, shaving the dorsum of the mouse and exposing the skin. Mice received a 30% total body surface area partial-thickness burn on the shaved dorsum, with approximate measurements 2 cm  $\times$  2 cm  $\times$  3 cm heated to 60 °C in a water bath for 17 s.

### 2.4. Isolation and characterization of TMPCs

On day 7 post-operation, murine TMPCs were harvested from the tendon insertion into the calcaneus to the distal gastrocnemius encompassing areas of THO formation and surrounding soft tissue, as previously described [20–22]. All collected tissues were mechanically dissociated using sterile scissors. Tissues were digested for 120 min in a solution of 300 U/mL of collagenase type II (Biosharp, Hefei, China) at 37 °C under sustained agitation. Samples were filtered using consecutive 70- $\mu$ m and 40- $\mu$ m sterile strainers, and digestion was quenched using equal parts standard growth medium (Cyagen, Suzhou, China) to generate a single-cell suspension. Cells were centrifuged at 1000 rpm for 5 min before removing the supernatant and washing in PBS. The cells were resuspended in standard growth media and subsequently plated at a density of  $1 \times 10^6$  cells/well in 6-well tissue culture plates. To characterize TMPCs, flow cytometry was performed for several stromal cell markers using the Mouse Mesenchymal Stem Cell Characterization Kit (Cyagen). As described in subsequent sections, the isolated cells were also tested for their chondrogenic and osteogenic differentiation

potential. Then, the TMPCs in passages 3–5 were used in the following experiments.

### 2.5. Evaluation of TMPCs proliferation

Colony forming unit (CFU) assay and 5-ethynyl-2'-deoxyuridine (p;[] incorporation assay were employed to assess the proliferation of TMPCs. For the CFU assay, TMPCs were plated at a density of  $1 \times 10^4$  cells/well in 6-well tissue culture plates for 10 days without changing the standard growth medium. DAPT/DMSO-treated cultures were grown in the standard growth medium for 3 days and then supplemented with DAPT (10  $\mu$ M) or DMSO vehicle for an additional 7 days. On day 10 after plating, cells were fixed for crystal violet staining. Type I colonies (CFU-F) were counted as previously described [8].

EdU incorporation assay was performed according to the manufacturer's instructions (Beyotime Biotechnology, Beijing, China). Briefly, cells were seeded in a 6-well plate at a density of  $1 \times 10^4$  cells/well and incubated with DAPT (10  $\mu$ M) or DMSO vehicle. After culture for 48 h, cells were exposed to 10  $\mu$ M EdU reagent for 2 h, then fixed with 4% paraformaldehyde, permeabilized with 0.5% Triton X-100, and stained with a Click-iT reaction cocktail. The cell nuclei were marked with Hoechst at a concentration of 5  $\mu$ g/mL for 30 min. The ratio of EdU-positive cells was calculated as the positive staining cells/the total cells  $\times$  100% using the ImageJ software 1.8.

### 2.6. Chondrogenic and osteogenic differentiation assay

The chondrogenesis and osteogenesis were induced by chondrogenic or osteogenic induction medium (Cyagen) for mouse BMSC. For chondrogenic differentiation, TMPCs ( $4 \times 10^5$  cells) were suspended in 500  $\mu$ L of chondrogenic differentiation media, then placed in a 15-ml tube and centrifuged at 250 g for 4 min allowing the cells to form a loose chondrocyte pellet (day 0). For osteogenic differentiation, TMPCs ( $1 \times 10^6$  cells/well) were seeded in 6-well plates (day 0) with a 2 ml osteogenic induction medium. The pellet or cells were incubated at 37 °C, 5% CO<sub>2</sub> and media changes were performed every 3 days. During induction, the pellet or cells were exposed to DAPT (10  $\mu$ M) for 5 or 14 days while a control group received DMSO only [23]. On day 14, the pellets after chondrogenic induction were harvested, and the expression of chondrogenic-related markers, including SOX9, COL2A1, and ACAN were assessed by western blot. The expression of osteogenic-related markers, including ALP, OCN, and Runx2 were also assessed in the cells after osteogenic induction. On day 21, Safranin O of the pellets were used to depict the degree of chondrogenesis after chondrogenic induction and Alizarin red staining of the cells were performed to measure mineral deposition after osteogenic induction. The percentage of positive areas was calculated as the positive staining area/the total image area  $\times$  100% using the ImageJ software 1.8.

### 2.7. Quantitative RT-PCR

Total RNA was extracted from the tissues, pellets or cells using RNAPure Tissue&Cell Kit (CWBI0, Taizhou, China), according to the manufacturer's instructions. And the RT-PCR for mRNAs was performed on a StepOne™ Real-Time PCR System (Thermo Scientific, MA, USA) using ChamQ Universal SYBR qPCR Master Mix (Vazyme, Nanjing, China). The PCR primer sequences of *Hes1*, *Hey1*, *Hey2*, *HeyL* and housekeeping gene GAPDH are shown in Supplemental Table S2. The relative expression levels of target genes were normalized to GAPDH and calculated using the  $2^{-\Delta\Delta Ct}$  method.

### 2.8. Western blot analysis

Total protein was extracted from chondrocyte pellets or cells using RIPA (Baiqiandu) following the manufacturer's protocol. Protein samples were loaded onto a 5% sodium dodecyl sulfate-polyacrylamide gel

electrophoresis and transferred to polyvinylidene fluoride membranes (Millipore, MA, USA). The membranes were blocked in 5% nonfat dry milk (Baiqiandu) in tris buffered saline tween (TBST, Baiqiandu) buffer for 1 h at 25 °C and then incubated at 4 °C overnight with monoclonal antibodies to detect SOX9, COL2A1, ACAN, ALP, OCN, and Runx2. In addition, GAPDH was used as an internal control. The relevant information about all primary antibodies is listed in Supplemental Table S3. The labeled protein bands were visualized using an Enhanced Chemiluminescence Detection Kit (Baiqiandu) and analyzed with ImageJ software 1.8. The relative levels of the target proteins were normalized to GAPDH.

### 2.9. DAPT administration in vivo

Forty mice were used to test the effect of gamma-secretase inhibition by DAPT on THO. Starting on postoperative day 1, mice were administered 50 mg/kg/day of freshly prepared DAPT (Selleck, TX, USA) dissolved in DMSO through intraperitoneal injections for 1 (n = 15) or 3 (n = 10) consecutive weeks [24]. A control group (n = 15) received DMSO only. Animals were sacrificed and the left hind limbs were harvested at different time points for the following histological or micro-CT examinations.

### 2.10. EdU incorporation assay in vivo

At 1 week after surgery, the mice in the DAPT (1-week administration) and control groups (n = 5 each) were anesthetized and then sacrificed. To test whether DAPT could inhibit TMSC proliferation *in vivo*, 5 mg/ml EdU dissolved in PBS was given to mice via intravenous injection 12 h prior to tissue collection. The left hind limbs were collected and fixed in 4% paraformaldehyde and then decalcified in 0.5 M EDTA at 4 °C. EdU fluorescence was detected as described above.

### 2.11. Histological analysis for ectopic cartilage and bone formation

At 3 weeks after surgery, 5 mice in each group were sacrificed, and the left hind limbs were collected followed by SafraninO/Fast Green staining to evaluate cartilage formation with a kit (Baiqiandu). At 9 weeks after surgery, 5 mice in each group were sacrificed and the left hind limbs were collected and processed for Masson's Trichrome staining to evaluate the bone formation with a kit (Baiqiandu). The ectopic cartilage and bone areas were morphometrically analyzed as mentioned above.

### 2.12. Micro-CT analysis for ectopic bone formation

At 9 weeks after surgery, the left hind limbs and the right femurs of mice in each group were scanned using a high-resolution micro-CT system (SkyScan 1176; Bruker microCT, Kontich, Belgium) to examine the volume of HO and the total bone mass, respectively (n = 5). Total new bone (differential new bone from native bone) formation in the left hind limbs was calculated using Bruker micro-CT volumetric software (version 1.14.10.0). For the right femurs, volume/tissue volume (BV/TV) and the number of trabeculae (TB.N) were analyzed to evaluate the total bone mass.

### 2.13. Statistical analysis

All relevant data are presented as mean  $\pm$  standard deviation (SD), and GraphPad Prism 7.0 (GraphPad Software., CA, USA) was used for data analysis. Student's t-test was employed to compare the quantitative data between the two groups. Comparisons among the groups were analyzed using the one-way ANOVA analysis of variance followed by Tukey's post hoc test. Statistical significance was assigned for  $P < 0.05$ .

### 3. Results

#### 3.1. The expressions of notch target genes were upregulated during THO formation

To determine if Notch signaling is involved in THO formation, the tissues from the insertion of the tendon into the calcaneus to the distal gastrocnemius were harvested from THO mice at 1, 3, 6 and 9 weeks post-surgery for quantitation of Notch target genes expressions. Normal tissues from healthy mice in the same sites served as a control. Real-time qPCR showed that the mRNA levels of *Hes1*, *Hey1*, *Hey2* and *HeyL* were upregulated at different stages of THO development (Fig. 1A–D). The expression of these genes peaked in the first week after surgery, then decreased but remained higher than genes in the normal control tissues. We further investigated the expressions of *Hey2* and *HeyL* by IHC in human THO specimens. A representative case of THO after Achilles tendon suture surgery is shown in Fig. 1E, demonstrating the ectopic bone within the Achilles tendon. HE staining after surgery further confirmed that the lesion was bone tissue (Fig. 1F). In the THO tissues, the immunoreactivities of *Hey2* and *HeyL* were stronger in the nucleus than those in the normal tissues (Fig. 1G and H).

#### 3.2. TMPCs expressed stromal cell markers and exhibited the chondrogenic and osteogenic differentiation potential

The morphology of TMPCs isolated from the injury tissues of the HO

model is shown in Fig. 2A. Flow cytometry revealed that these cells expressed CD44, CD90, CD29 and Sca-1 but did not express CD117 and CD31 (Fig. 2B). In addition, consistent with previous studies [20–22], we demonstrated that the cells could differentiate into chondrocytes and osteoblasts under a chondrogenic or osteogenic induction medium over 21 days, respectively (Fig. 2C and D).

#### 3.3. Sustained administration of DAPT restricted TMPCs proliferation in vitro

TMPCs were cultured to assay the frequency of fibroblastic colony-forming units (CFU-Fs). After 7 days of culture, crystal violet staining of DAPT-treated cells showed a dramatic reduction in CFU colonies compared with that in DMSO-treated controls ( $P < 0.001$ ; Fig. 3A and B). Then, we performed EdU staining further to gauge the effects of DAPT on cell proliferation. Results showed that the number of EdU-positive cells in the DAPT group was less than in the control group after 48 h of culture ( $P < 0.001$ ; Fig. 3C and D).

#### 3.4. Sustained administration of DAPT represses TMPCs chondrogenic differentiation in vitro

To determine whether DAPT affects the chondrogenic differentiation of TMPCs, we cultured TMPCs with 14-day DAPT, 5-day DAPT or DMSO under chondrogenic differentiation conditions. Cartilage matrix deposition of chondrocyte pellets was measured by Safranin-O staining after 21

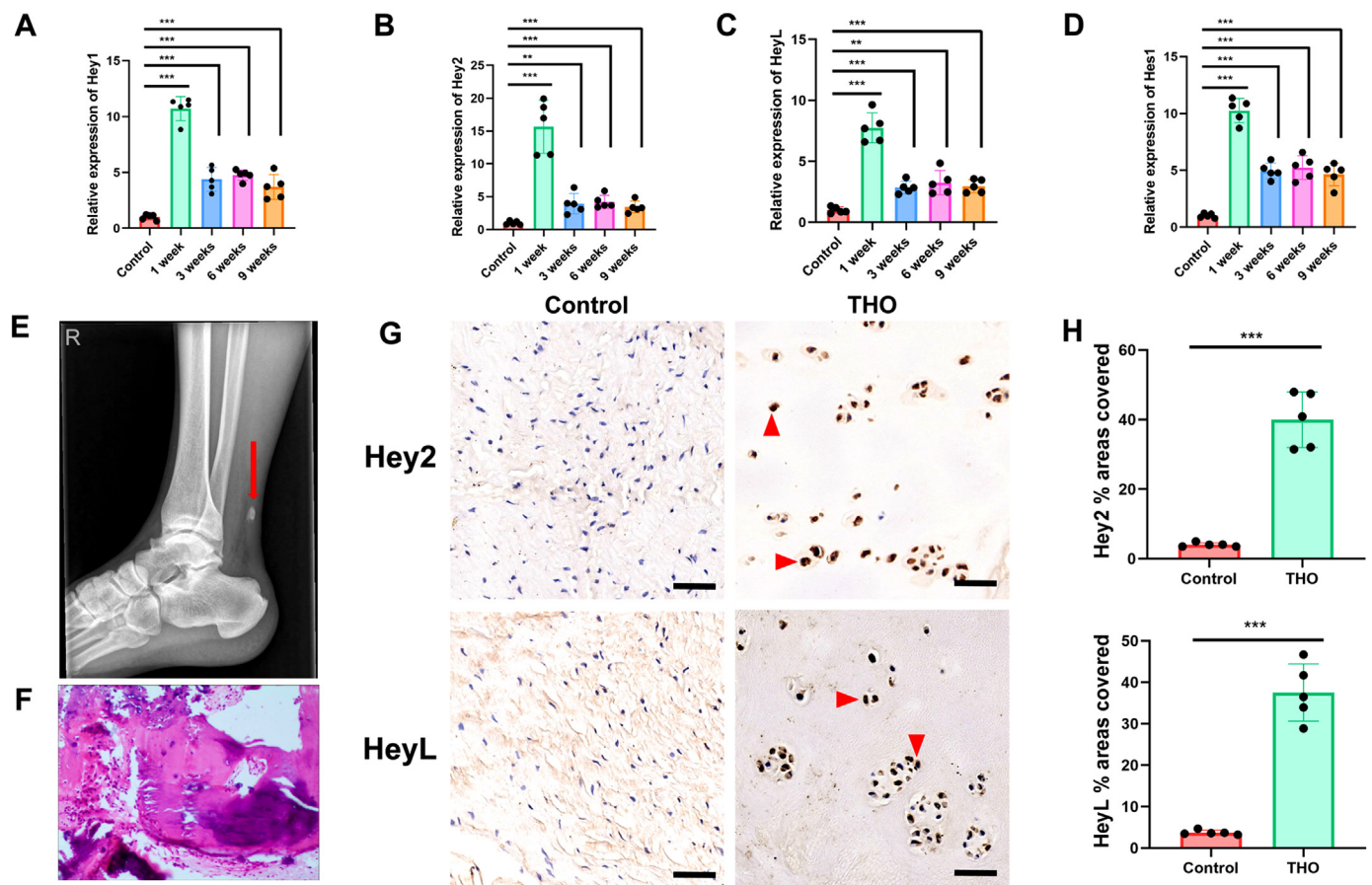


**Fig. 1. Notch target genes expressions were upregulated in mice and human THO tissues** (A–D) Quantitative RT-PCR results of Notch target genes expressions in mice THO and corresponding normal tissues (control) at 1, 3, 6 and 9 weeks post-surgery ( $n = 5$ ) (E) X-ray film image of a representative case of THO. The red arrow indicates ectopic bone within the soft tissue (F) H&E-stained image of the surgically resected THO lesion in Figure E (G) IHC images of *Hey2* or *HeyL* localization in human THO and normal tissues. Red arrowheads indicate *Hey2* or *HeyL* (brown) expression in the nucleus (H) Quantification of the average immunoreactivity intensity of *Hey2* and *HeyL* in the nucleus ( $n = 5$ ). Scale bar = 50  $\mu\text{m}$   $**P < 0.01$ , and  $***P < 0.001$ . (For interpretation of the references to color in this figure legend, the reader is referred to the Web version of this article.)

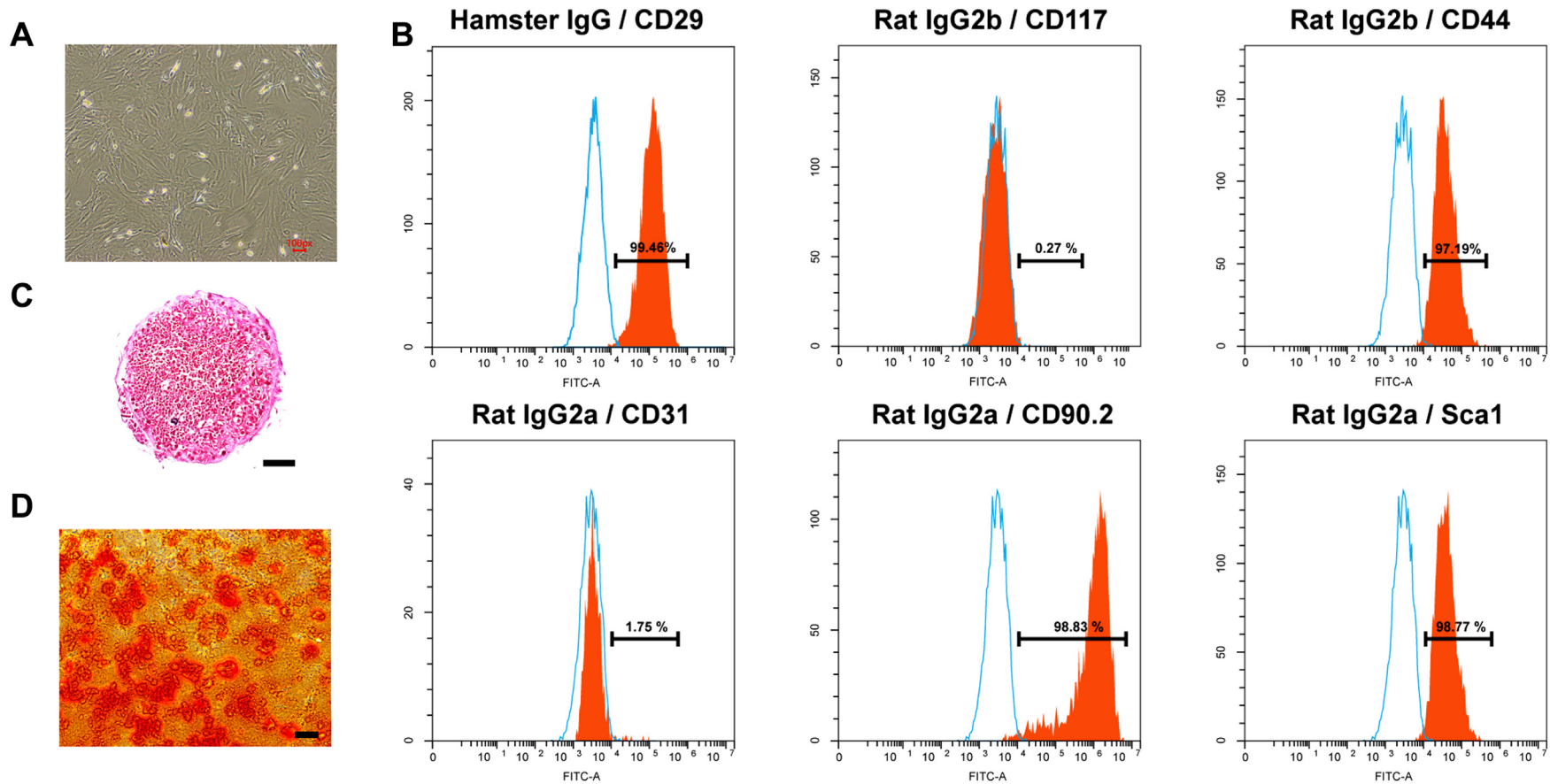


**Fig. 2.** TMPCs expressed stromal cell markers and exhibited the chondrogenic and osteogenic differentiation potential (A) The morphology of TMPCs (B) The specific surface markers of TMPCs analyzed by flow cytometry (n = 3) (C) Safranin-O staining of TMPCs pellets under a chondrogenic induction medium over 21 days (n = 3) (D) Alizarin red staining of TMPCs under an osteogenic induction medium over 21 days (n = 3). Scale bar = 100  $\mu$ m. (For interpretation of the references to color in this figure legend, the reader is referred to the Web version of this article.)

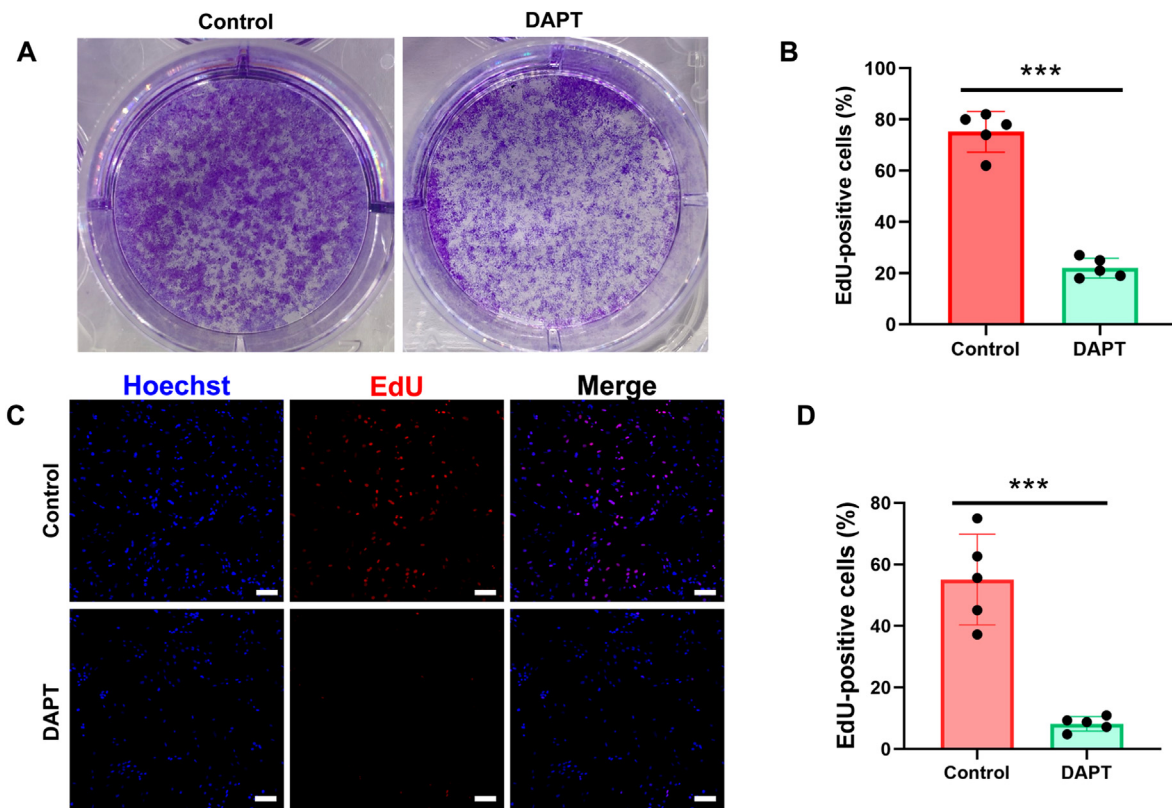


**Fig. 3. Sustained administration of DAPT reduced TMPCs proliferation *in vitro*** (A) The crystal violet staining results of CFU-F assays for TMPCs treated with either DMSO or DAPT for 7 days (B) The number of type I colonies (CFU-Fs) was quantified from CFU-F assays ( $n = 3$ ) (C) EdU incorporation assay results for TMPCs treated with either DMSO or DAPT for 48 h (Red = EdU; Blue = DAPI) (D) The percentage of EdU-positive cells versus total cells from EdU incorporation assay ( $n = 3$ ). \*\*\* $P < 0.001$ . Scale bar = 100  $\mu\text{m}$ . (For interpretation of the references to color in this figure legend, the reader is referred to the Web version of this article.)

days of chondrogenic induction. The intensity of Safranin-O staining was lower (indicative of poor proteoglycan contents) in pellets in the DAPT groups than that in the control group (both  $P < 0.001$ ; Fig. 4A and B). In addition, the longer the duration of DAPT administration, the stronger the inhibition of the formation of proteoglycan contents under chondrogenic differentiation. Western blot results also showed that DAPT triggered the time-dependent down-regulation of expressions of typical chondrogenic-specific markers, including SOX9, COL2A1, and ACAN in TMPCs after 28 days of chondrogenic induction (Fig. 4C–F). The expressions of Notch target gene including Hey2 and HeyL, were also significantly lower in pellets cultured with DAPT than DMSO, indicating that Notch target gene was successfully suppressed by DAPT (Fig. 4G–I). Together, these findings highlight a negative role of Notch signaling inhibition with DAPT on the chondrogenic differentiation of TMPCs.

### 3.5. Sustained administration of DAPT represses TMPCs osteogenic differentiation *in vitro*

We further investigated the effect of DAPT on TMPCs osteogenic differentiation. Alizarin red staining performed at day 21 of differentiation confirmed a reduction in mineralization of TMPCs treated with DAPT compared with DMSO ( $P < 0.001$ ; Fig. 5A and B). In addition, the longer the duration of DAPT administration, the stronger the inhibition of mineralization under osteogenic differentiation. Western blot results also showed that DAPT triggered the time-dependent down-regulation of expressions of typical osteogenic-specific markers, including ALP, Runx2 and OCN (Fig. 5C–F). The expressions of Notch target gene including Hey2 and HeyL, were also significantly lower in cells cultured with DAPT than DMSO, indicating that Notch target gene was successfully suppressed by DAPT during osteogenic differentiation (Fig. 5G–I). Together, these results suggest that Notch signaling inhibition with DAPT

significantly represses the osteogenic differentiation of TMPCs.

### 3.6. DAPT treatment reduced TMPCs proliferation *in vivo*

To evaluate the effects of DAPT on TMPCs proliferation *in vivo*, the EdU solution was given to mice 12 h before tissue collection at 1 week after surgery. DAPT-treated mice showed a significant decrease in the number of EdU-positive cells inside the lesion tissues of the left hind limbs compared with control mice, demonstrating a smaller proliferation index ( $P < 0.001$ , Fig. 6A and B). The results further indicated that DAPT could inhibit cell proliferation in the lesion site, including TMPCs.

### 3.7. Sustained DAPT treatment inhibits ectopic cartilage and bone formation *in vivo*

To characterize the effects of sustained Notch inhibition on THO formation *in vivo*, we firstly analyzed the lesion tissue sections at 3 weeks post-surgery via Safranin O/Fast Green staining for ectopic cartilage formation (Fig. 7A). In the 3-week ( $0.0627 \pm 0.0461 \text{ mm}^2$ ) and the 1-week ( $0.2525 \pm 0.0246 \text{ mm}^2$ ) DAPT groups, we detected a significant decrease in cartilage areas compared to the control group ( $0.7808 \pm 0.0393 \text{ mm}^2$ ) (both  $P < 0.001$ ; Fig. 7B). Secondly, Masson's trichrome staining on samples 9 weeks after tenotomy was used to highlight the ectopic bone matrix, which was likewise less conspicuous in the DAPT-treated animals (Fig. 7C). Micro-CT again demonstrated the less ectopic bone volume in the 3-week ( $0.1173 \pm 0.07036 \text{ mm}^3$ ) and 1-week DAPT ( $0.4644 \pm 0.1422 \text{ mm}^3$ ) groups than that in the control group ( $1.058 \pm 0.3142 \text{ mm}^3$ ) ( $P < 0.001$  and  $P < 0.05$  respectively; Fig. 7D and E). In addition, the longer the duration of DAPT application, the more potent inhibition of the ectopic cartilage and bone formation. Finally, to test the effect of DAPT administration on total body bone mass, we

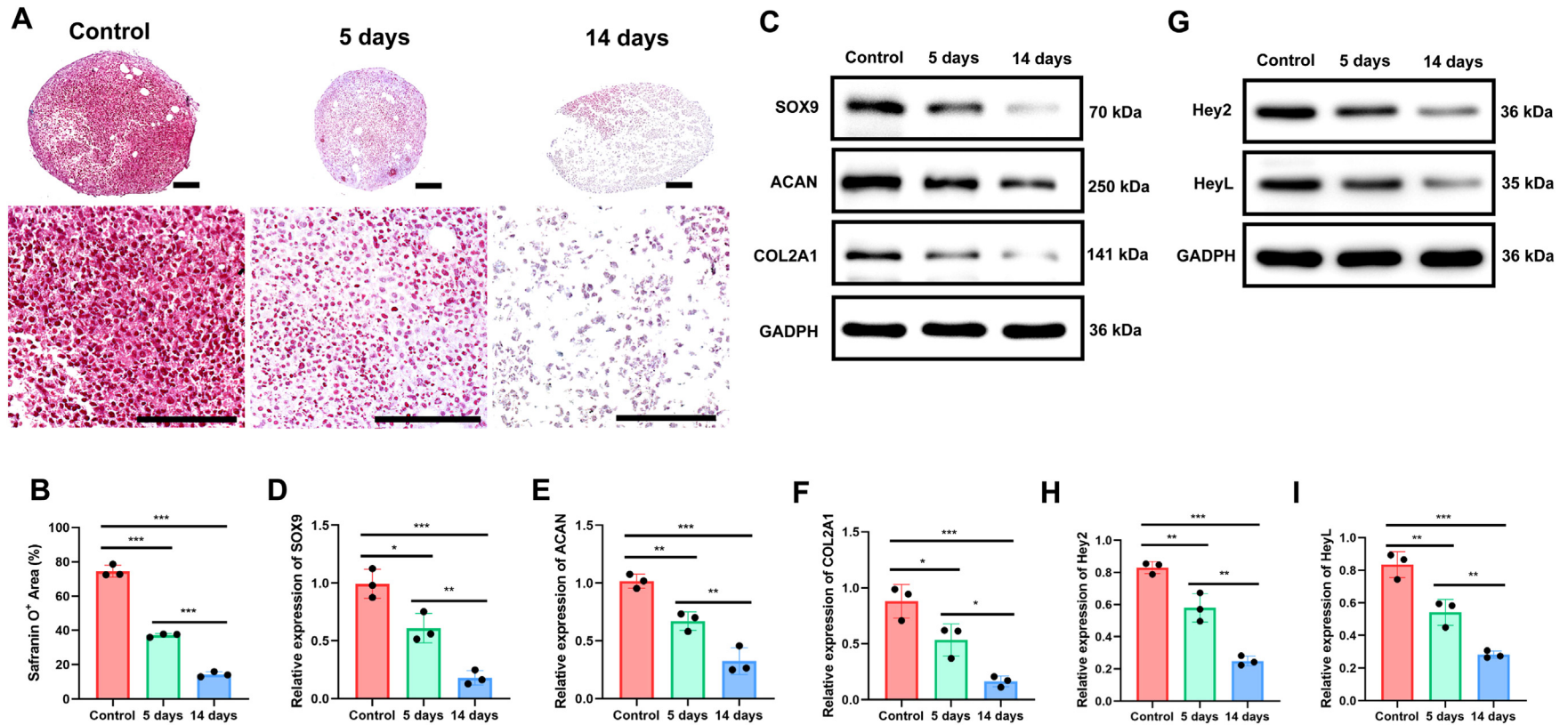


**Fig. 4. Sustained administration of DAPT inhibits TMPCs chondrogenic differentiation *in vitro*** (A) Safranin-O staining images of chondrocyte pellets after chondrogenic induction in control, 5-day and 14-day DAPT groups. Original magnification:  $\times 10$  (top row);  $\times 20$  (bottom row) (B) Quantification of the intensity of Safranin-O staining in different groups (C) Western blot analyses of the expressions of chondrogenic-related markers during TMPCs chondrogenic differentiation (D–F) Quantification of the expressions of chondrogenic-related markers assessed by western blot (G) Western blot analyses of the expressions of the Notch target genes during TMPCs chondrogenic differentiation (H, I) Quantification of the expressions of Notch target genes assessed by western blot. \* $P < 0.05$ , \*\* $P < 0.01$ , \*\*\* $P < 0.001$ . Scale bar: 100  $\mu\text{m}$ .

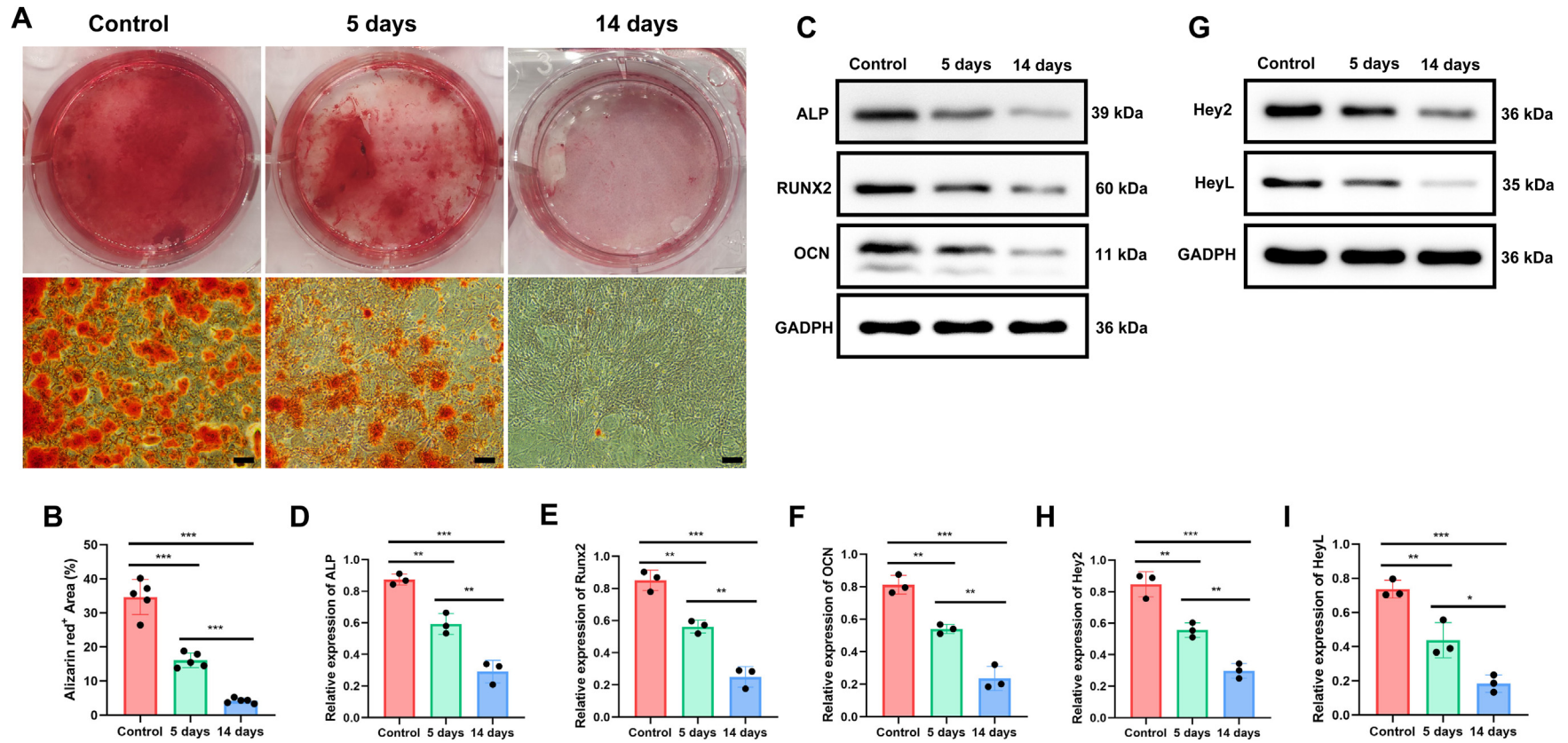


**Fig. 5. Sustained administration of DAPT represses TMPCs osteogenic differentiation *in vitro*** (A) Alizarin red staining of TMPCs after osteogenic induction in control, 5-day and 14-day DAPT groups (B) Quantification of Alizarin Red S positive areas in different groups (C) Western blot analyses of the expressions of osteogenic-specific markers during TMPCs osteogenic differentiation (D–F) Quantification of the expressions of osteogenic-specific markers assessed by western blot (G) Western blot analyses of the expression of osteogenic-specific marker and Notch target genes during TMPCs osteogenic differentiation (H, I) Quantification of the expressions of Notch target genes assessed by western blot. \* $P < 0.05$ , \*\* $P < 0.01$ , \*\*\* $P < 0.001$ . Scale bar: 100  $\mu\text{m}$ . (For interpretation of the references to color in this figure legend, the reader is referred to the Web version of this article.)



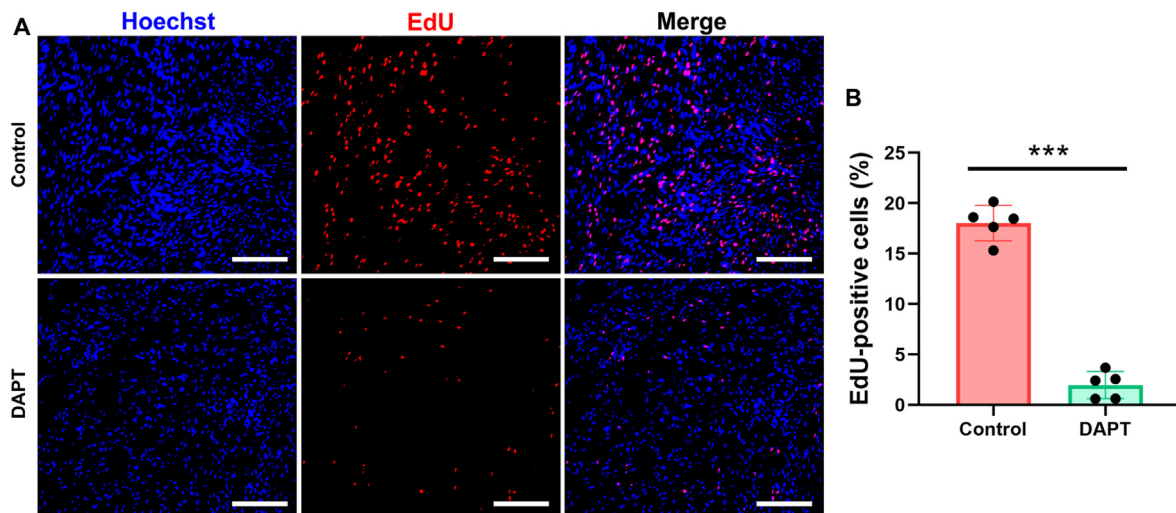


**Fig. 6.** DAPT treatment reduced TMPCs proliferation *in vivo* (A) EdU staining of the lesion tissues collected from control and DAPT-treated mice (Red = EdU; Blue = DAPI) (B) Quantification of the percentage of EdU-positive cells. \*\*\* $P < 0.001$ . Scale bar: 100  $\mu\text{m}$ . (For interpretation of the references to color in this figure legend, the reader is referred to the Web version of this article.)

scanned the right femurs of the THO models (Fig. 7F) and found no significant difference in the bone volume/tissue volume and trabecular number among the three groups (Fig. 7G and H).

#### 4. Discussion

The Notch signaling pathway is known to regulate cell proliferation, differentiation, cell fate determination, and stem/progenitor cell self-renewal in both embryonic and adult organs [25]. Pharmacological disruption of Notch signaling using a gamma-secretase inhibitor has proven to have beneficial effects on a variety of healing systems, and several gamma-secretase inhibitors are now being used in clinical trials primarily focused on various types of cancer and Alzheimer's disease [26, 27]. In the current study, we demonstrated for the first time that the expressions of genes associated with canonical Notch signaling were upregulated during THO formation. By using the gamma-secretase inhibitor DAPT, we revealed that blocking NOTCH signaling could inhibit proliferation, chondrogenic and osteogenic differentiation of TMPCs from the THO lesion sites *in vitro*, and lead to decreased ectopic cartilage and bone formation in the mouse THO model. To our knowledge, these findings uncover new pathways and therapeutic targets for THO.

Previous studies have implicated an activated Notch signaling on embryological bone development and fracture repairing in mice and humans [28,29]. The mechanisms of THO formation are believed to recapitulate a series of spatiotemporal cellular and signaling events that occur during skeletal development [4], suggesting a potential involvement of NOTCH signaling. In our mouse THO models, the expressions of Notch target genes including *Hes1*, *Hey1*, *Hey2* and *HeyL*, are significantly higher in THO lesions relative to healthy tissues. Furthermore, the animal experiment results were also verified in human THO specimens. These findings demonstrated that the Notch pathway might also play a crucial facilitating role in THO formation and targeting the Notch signaling pathway might ultimately provide a mechanism to inhibit the formation of THO.

During the formation of THO, TMPCs are recruited to the injury site of the Achilles's tendon and undergo chondrogenesis to produce an initial cartilaginous callus [20–22]. In this regard, we focused on TMPCs rather than the more commonly used bone mesenchymal progenitor cells. Although previous studies have confirmed that DAPT played complicated roles in chondrogenesis and osteogenesis in other cell types, such as murine ATDC5 and C3H10T1/2 cells [30,31], TMPCs exhibit some epigenetic and transcriptional distinctions with these osteochondrogenic

progenitors [21]. These distinctions could also affect the responsiveness of Notch pathway inhibition, whether genetically or pharmacologically, on proliferation, chondrogenic and osteogenic differentiation.

Transient gamma-secretase inhibition by DAPT could accelerate and enhance fracture repair via Notch signaling modulation, which is partially due to the early enhancement chondro-osteogenic transition in local mesenchymal progenitor cells [24]. However, sustained Notch signaling inhibition will reduce proliferation and exhaust the progenitor pool of MSCs correlating with bone fracture repair [32–34]. In the present study, we observed that TMPCs treated with DAPT showed impaired proliferation capability compared with control cells *in vitro*. The *in vivo* experiments further confirmed that DAPT could inhibit cell proliferation in the lesion site, including TMPCs. As cell proliferation is associated with increased ossification [35], we reasoned that the reduced THO formation observed in sustained DAPT-treated mice might be partly due to the TMPCs exhaustion.

Although inhibition of the Notch pathway may increase the transition of TMPCs from one phase to the next and lead to increased cell numbers for chondro-osteogenic differentiation, the Notch pathway plays a context-dependent function at different time points within a cell lineage during the process of endochondral ossification. The present data suggested that sustained DAPT incubation decreased the extracellular matrix production of the chondrogenic pellets, accompanied by reduced expressions of chondrogenic marker genes under the chondrogenesis induction. A previous study investigating human MSCs in monolayer culture showed that blocking Notch activation with DAPT inhibited chondrogenic differentiation [36]. Moreover, the JAG1 mediated Notch signaling was revealed with DAPT to be necessary for chondrogenesis of hMSCs, as inhibition days 0–14, or just days 0–5, blocked chondrogenesis, whereas Notch inhibition days 5–14 did not [15]. These results indicated that the early transient Notch activation in chondrogenic progenitors provided crucial signals before full chondrogenesis could proceed. Our research found that when Notch signaling was inhibited sustainedly, chondrogenesis could be repressed. In addition, we also observed that sustained DAPT treatment impaired osteogenic differentiation of TMPCs, which was consistent with several previous reports indicating that the inhibition of Notch signaling impaired *in vitro* osteogenic differentiation from various progenitor and immature cell types [18,37,38]. These observations highlight that the reduced THO formation by sustained DAPT treatment might also be partly ascribed to the significant inhibition of chondrogenic and osteogenic differentiation in TMPCs. Moreover, the longer the duration of DAPT administration, the

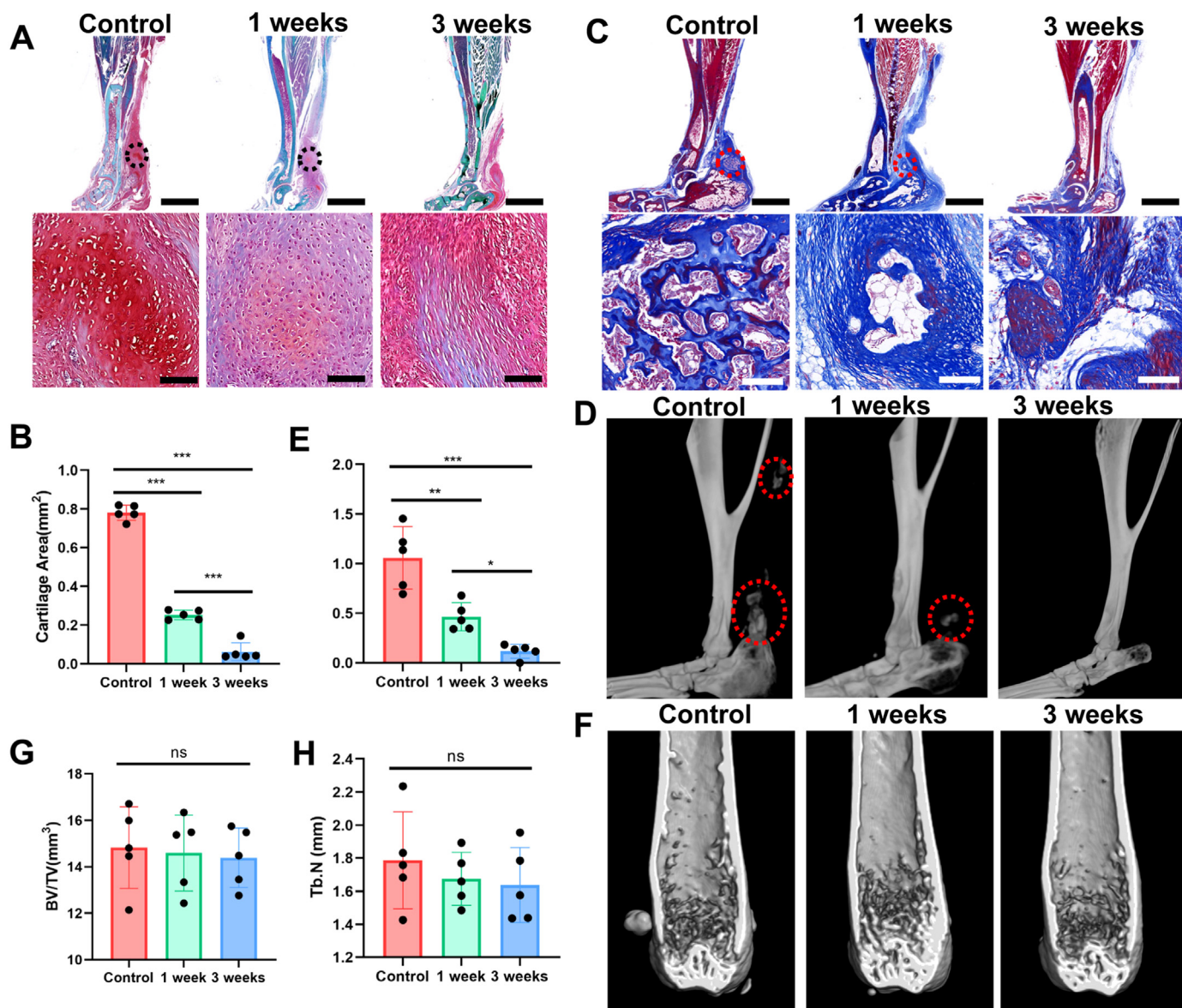


**Fig. 7. Sustained DAPT treatment inhibits ectopic cartilage and bone formation in THO model mice** (A) Representative Safranin O red/fast green staining images within the lesion site from control, 1-week DAPT and 3-week DAPT groups at 3 weeks after tenotomy. The ectopic cartilage appears orange (black circle). Original magnification:  $\times 1$  (scale bar: 2 mm; top row);  $\times 20$  (scale bar: 100  $\mu\text{m}$ ; bottom row) (B) Histomorphometry quantifications of ectopic cartilage areas in the lesion sites ( $n = 5$ ) (C) Masson's trichrome staining within the lesion site from different groups 9 weeks after tenotomy. The ectopic bone appears dark blue (red circle). Original magnification:  $\times 1$  (scale bar: 2 mm; top row);  $\times 20$  (scale bar: 100  $\mu\text{m}$ ; bottom row) (D) Micro-CT reconstruction images of ectopic bone formation (red circle) from different groups at 9 weeks after tenotomy (E) Micro-CT quantifications of ectopic bone volume in the lesion sites ( $n = 5$ ) (F) Micro-CT reconstruction images of the right femurs from different groups at 9 weeks after tenotomy (G, H) Micro-CT quantifications of femoral bone volume/tissue volume (BV/TV) and trabecular numbers (Tb. N) ( $n = 5$ ). ns = not significant.  $*P < 0.05$ ,  $**P < 0.01$ ,  $***P < 0.001$ . (For interpretation of the references to color in this figure legend, the reader is referred to the Web version of this article.)

stronger the inhibition of chondrogenic and osteogenic differentiation.

To confirm the effect of NOTCH signaling inhibiting in the context of THO *in vivo*, we treated THO mice models with DAPT. Previous studies have demonstrated that the Notch gene mutation is responsible for Hajdu-Cheney syndrome which causes osteoporosis in humans [28] and deletion of the dominant ligand-Jag1, dysregulates the osteochondral progenitor cell pool and produces femoral trabecular osteopenia in adulthood [12]. In order to evaluate which regime would be safer and more effective in THO treatment, we investigated two dosing strategies: 1-week and 3-week doses of 50 mg/kg of DAPT. It is of note that the most obviously reduced ectopic cartilage and bone formation observed during THO development with sustained 3-week DAPT treatments, which extends well into the early cartilage formation phase [5,39], could be

caused by combined effects from the loss of Notch signaling in both the TMSC population and committed chondrocytes in the cartilaginous lesions. Moreover, DAPT administration within 3 weeks did not result in a decrease in total bone mass. Therefore, collectively our data suggest that long-term sustained Notch inhibition appears to be preferential to short-term sustained Notch inhibition to achieve an appropriate balance of reduced THO formation.

Our study had several limitations. First, DAPT is a specific gamma-secretase inhibitor, but the function of such enzymes is not exclusive to the Notch pathway [40]. We therefore cannot conclude that all the effects we observed are solely due to Notch signaling inhibition. Another limitation is that TMPCs may not be the sole source of cells contributing to THO at the injury site. Several other cell types, such as immune and

endothelial cells, have been implicated in THO formation [1]. Further studies are necessary to assess the effect of DAPT on other cell types associated with THO. Finally, we only set one dose and used DAPT within 3 weeks. Whether longer application or higher doses of the DAPT has better therapeutic effect or cause side effects has not been studied. Therefore, future researches are warranted to investigate these problems to accelerate the clinical application of DAPT in THO treatment.

## 5. Conclusion

In conclusion, we have demonstrated that the expressions of several Notch target genes are upregulated in mice and human THO lesions, indicating activated Notch signaling. This activation induces and represses the transcription of genes that may potentially contribute to THO. Sustained Notch signaling inhibition by the gamma-secretase inhibitor-DAPT reduced TMPCs proliferation and osteogenic and chondrogenic differentiation in a time-dependent manner, as well as inhibited ectopic cartilage and bone formation in a mouse THO model. Our findings presented here raise the possibility that sustained Notch inhibition via systemic DAPT (or other similar gamma-secretase inhibitors) administration has promising clinical utility for inhibiting THO formation, providing new insight into THO prophylaxis and treatment.

## Conflicts of interest

The authors declare no conflicts of interest.

## Author contribution

Conception and design of study: W Zheng, A.X Yu, Z.H Li, Q.Y Liu, acquisition of data: W Zheng, X.Z.Y Yi, C Jian, B.W Qi, analysis and/or interpretation of data: W Zheng, X.Z.Y Yi, A.X Yu, Z.H Li, Q.Y Liu, Drafting the manuscript: W Zheng, X.Z.Y Yi, revising the manuscript critically for important intellectual content: A.X Yu, Z.H Li, Q.Y Liu, Approval of the version of the manuscript to be published (the names of all authors must be listed): W Zheng, X.Z.Y Yi, C Jian, B.W Qi, Q.Y Liu, Z.H Li, A.X Yu, Acknowledgements.

## Acknowledgements

This work was supported by the Health Commission of Hubei Province Medical Leading Talent Project (no. LJ20200405).

## Appendix A. Supplementary data

Supplementary data to this article can be found online at <https://doi.org/10.1016/j.jot.2023.06.004>.

## References

- Meyers C, Lisiecki J, Miller S, Levin A, Fayad L, Ding C, et al. Heterotopic ossification: a comprehensive review. *JBMR Plus* 2019;3:e10172.
- Ranganathan K, Loder S, Agarwal S, Wong VW, Wong VC, Forsberg J, et al. Heterotopic ossification: basic-science principles and clinical correlates. *J Bone Jt Surg Am* 2015;97:1101–11.
- Agarwal S, Loder S, Cholok D, Li J, Breuler C, Drake J, et al. Surgical excision of heterotopic ossification leads to re-emergence of mesenchymal stem cell populations responsible for recurrence. *Stem Cells Transl Med* 2017;6:799–806.
- Hwang C, Marini S, Huber AK, Stepien DM, Sorkin M, Loder S, et al. Mesenchymal VEGFA induces aberrant differentiation in heterotopic ossification. *Bone Res* 2019; 7:36.
- Agarwal S, Loder S, Brownley C, Cholok D, Mangiavini L, Li J, et al. Inhibition of Hif1alpha prevents both trauma-induced and genetic heterotopic ossification. *Proc Natl Acad Sci U S A* 2016;113:E338–47.
- Dey D, Bagarova J, Hatsell SJ, Armstrong KA, Huang L, Ermann J, et al. Two tissue-resident progenitor lineages drive distinct phenotypes of heterotopic ossification. *Sci Transl Med* 2016;8. 366ra163.
- Hosaka Y, Saito T, Sugita S, Hikata T, Kobayashi H, Fukai A, et al. Notch signaling in chondrocytes modulates endochondral ossification and osteoarthritis development. *Proc Natl Acad Sci U S A* 2013;110:1875–80.
- Hilton MJ, Tu X, Wu X, Bai S, Zhao H, Kobayashi T, et al. Notch signaling maintains bone marrow mesenchymal progenitors by suppressing osteoblast differentiation. *Nat Med* 2008;14:306–14.
- Mead TJ, Yutzey KE. Notch pathway regulation of chondrocyte differentiation and proliferation during appendicular and axial skeleton development. *Proc Natl Acad Sci U S A* 2009;106:14420–5.
- Zanotti S, Canalis E. Notch signaling and the skeleton. *Endocr Rev* 2016;37:223–53.
- Dishowitz MI, Terkorn SP, Bostic SA, Hankenson KD. Notch signaling components are upregulated during both endochondral and intramembranous bone regeneration. *J Orthop Res* 2012;30:296–303.
- Youngstrom DW, Dishowitz MI, Bales CB, Carr E, Mutyaba PL, Kozloff KM, et al. Jagged1 expression by osteoblast-lineage cells regulates trabecular bone mass and periosteal expansion in mice. *Bone* 2016;91:64–74.
- Youngstrom DW, Senos R, Zondervan RL, Brodeur JD, Lints AR, Young DR, et al. Intraoperative delivery of the Notch ligand Jagged-1 regenerates appendicular and craniofacial bone defects. *NPJ Regen Med* 2017;2:32.
- Oldershaw RA, Hardingham TE. Notch signaling during chondrogenesis of human bone marrow stem cells. *Bone* 2010;46:286–93.
- Oldershaw RA, Tew SR, Russell AM, Meade K, Hawkins R, McKay TR, et al. Notch signaling through Jagged-1 is necessary to initiate chondrogenesis in human bone marrow stromal cells but must be switched off to complete chondrogenesis. *Stem Cell* 2008;26:666–74.
- Pakvasa M, Haravu P, Boachie-Mensah M, Jones A, Coalsen E, Liao J, et al. Notch signaling: its essential roles in bone and craniofacial development. *Genes Dis* 2021; 8:8–24.
- Tu X, Chen J, Lim J, Karner CM, Lee S-Y, Heisig J, et al. Physiological notch signaling maintains bone homeostasis via RBPjk and Hey upstream of NFATc1. *PLoS Genet* 2012;8:e1002577.
- Novak S, Roeder E, Sinder BP, Adams DJ, Siebel CW, Grcevic D, et al. Modulation of Notch1 signaling regulates bone fracture healing. *J Orthop Res* 2020;38:2350–61.
- Peterson JR, Agarwal S, Brownley RC, Loder SJ, Ranganathan K, Cederna PS, et al. Direct mouse trauma/burn model of heterotopic ossification. *J Vis Exp* 2015: e52880.
- Agarwal S, Loder SJ, Sorkin M, Li S, Shrestha S, Zhao B, et al. Analysis of bone-cartilage-stromal progenitor populations in trauma induced and genetic models of heterotopic ossification. *Stem Cell* 2016;34:1692–701.
- Strong AL, Spreadborough PJ, Pagani CA, Haskins RM, Dey D, Grimm PD, et al. Small molecule inhibition of non-canonical (TAK1-mediated) BMP signaling results in reduced chondrogenic ossification and heterotopic ossification in a rat model of blast-associated combat-related lower limb trauma. *Bone* 2020;139:115517.
- Strong AL, Spreadborough PJ, Dey D, Yang P, Li S, Lee A, et al. BMP ligand trap ALK3-Fc attenuates osteogenesis and heterotopic ossification in blast-related lower extremity trauma. *Stem Cell Dev* 2021;30:91–105.
- Ichida JK, Tcw J, Williams LA, Carter AC, Shi Y, Moura MT, et al. Notch inhibition allows oncogene-independent generation of iPSC cells. *Nat Chem Biol* 2014;10: 632–9.
- Wang C, Shen J, Yukata K, Inzana JA, O'Keefe RJ, Awad HA, et al. Transient gamma-secretase inhibition accelerates and enhances fracture repair likely via Notch signaling modulation. *Bone* 2015;73:77–89.
- Zhou B, Lin W, Long Y, Yang Y, Zhang H, Wu K, et al. Notch signaling pathway: architecture, disease, and therapeutics. *Signal Transduct Targeted Ther* 2022;7:95.
- Lee J-H, Ostalecki C, Oberstein T, Schierer S, Zinser E, Eberhardt M, et al. Alzheimer's disease protease-containing plasma extracellular vesicles transfer to the hippocampus via the choroid plexus. *EBioMedicine* 2022;77:103903.
- Yang X, Zhang Y, Huang Y, Wang Y, Qi X, Su T, et al. Evodiamine suppresses Notch3 signaling in lung tumorigenesis via direct binding to  $\gamma$ -secretases. *Phytomedicine* 2020;68:153176.
- Isidor B, Lindenbaum P, Pichon O, Bézieau S, Dina C, Jacquemont S, et al. Truncating mutations in the last exon of NOTCH2 cause a rare skeletal disorder with osteoporosis. *Nat Genet* 2011;43:306–8.
- Dishowitz MI, Terkorn SP, Bostic SA, Hankenson KD. Notch signaling components are upregulated during both endochondral and intramembranous bone regeneration. *J Orthop Res* 2012;30:296–303.
- Kohn A, Dong Y, Mirando AJ, Jesse AM, Honjo T, Zuscik MJ, et al. Cartilage-specific RBPjkappa-dependent and -independent Notch signals regulate cartilage and bone development. *Development* 2012;139:1198–212.
- Ying J, Xu T, Wang C, Jin H, Tong P, Guan J, et al. Dnmt3b ablation impairs fracture repair through upregulation of Notch pathway. *JCI Insight* 2020;5:e131816.
- Wang C, Inzana JA, Mirando AJ, Ren Y, Liu Z, Shen J, et al. NOTCH signaling in skeletal progenitors is critical for fracture repair. *J Clin Invest* 2016;126:1471–81.
- Dishowitz MI, Mutyaba PL, Takacs JD, Barr AM, Engiles JB, Ahn J, et al. Systemic inhibition of canonical Notch signaling results in sustained callus inflammation and alters multiple phases of fracture healing. *PLoS One* 2013;8:e68726.
- Oldershaw RA, Hardingham TE. Notch signaling during chondrogenesis of human bone marrow stem cells. *Bone* 2010;46:286–93.
- Yan M, Duan X, Cai L, Zhang W, Silva MJ, Brophy RH, et al. KIF26B silencing prevents osseous transdifferentiation of progenitor/stem cells and attenuates ectopic calcification in a murine model. *J Bone Miner Res* 2022;37:349–68.
- Karlsson C, Jonsson M, Asp J, Brantsing C, Kageyama R, Lindahl A. Notch and HES5 are regulated during human cartilage differentiation. *Cell Tissue Res* 2007;327: 539–51.
- Wagley Y, Chesi A, Acevedo PK, Lu S, Wells AD, Johnson ME, et al. Canonical Notch signaling is required for bone morphogenetic protein-mediated human osteoblast differentiation. *Stem Cell* 2020;38:1332–47.
- AlMuraikhi N, Ali D, Vishnubalaji R, Manikandan M, Attaya M, Siyal A, et al. Notch signaling inhibition by LY411575 attenuates osteoblast differentiation and

- decreased ectopic bone formation capacity of human skeletal (mesenchymal) stem cells. *Stem Cell Int* 2019;3041262.
- [39] Hsu GC, Marini S, Negri S, Wang Y, Xu J, Pagani C, et al. Endogenous CCN family member WISP1 inhibits trauma-induced heterotopic ossification. *JCI Insight* 2020; 5:e135432.
- [40] Vujovic S, Henderson SR, Flanagan AM, Clements MO. Inhibition of gamma-secretases alters both proliferation and differentiation of mesenchymal stem cells. *Cell Prolif* 2007;40:185–95.